J. Appl. Math. & Informatics Vol. **28***(2010), No. 5 - 6, pp. 1055 - 1071*
Website: http://www.kcam.biz

AN EFFICIENT AND STABLE ALGORITHM FOR NUMERICAL EVALUATION OF HANKEL TRANSFORMS

OM P. SINGH*, VINEET K. SINGH AND RAJESH K. PANDEY

Abstract. Recently, a number of algorithms have been proposed for numerical evaluation of Hankel transforms as these transforms arise naturally in many areas of science and technology. All these algorithms depend on separating the integrand $rf(r)J_\upsilon(pr)$ into two components; the slowly varying component $rf(r)$ and the rapidly oscillating component $J_\upsilon(pr)$. Then the slowly varying component $rf(r)$ is expanded either into a Fourier Bessel series or various wavelet series using different orthonormal bases like Haar wavelets, rationalized Haar wavelets, linear Legendre multiwavelets, Legendre wavelets and truncating the series at an optimal level; or approximating $rf(r)$ by a quadratic over the subinterval using the Filon quadrature philosophy. The purpose of this communication is to take a different approach and replace rapidly oscillating component $J_\upsilon(pr)$ in the integrand by its Bernstein series approximation, thus avoiding the complexity of evaluating integrals involving Bessel functions. This leads to a very simple efficient and stable algorithm for numerical evaluation of Hankel transform.

AMS Mathematics Subject Classification : 41A10, 65R10.
Key words and phrases : Hankel Transform, Bernstein Polynomial, Random Noise.

1. Introduction

There are several integral transforms which are frequently used as a tool for solving numerous scientific problems. It is well known that the Fourier transform (FT) is used to obtain spatial spectrum of optical light [12]. Fourier optics is widely used in optical instrument design, optical propagation through lenses and in quadratics graded index mediums. Most classical optical systems like mirrors or lenses are axially symmetrical devices. In many practical problems, data are often acquired in such a form that it is desirable to perform a two-dimensional polar Fourier transform that is a Hankel transform (HT) rather

Received September 28, 2009. Revised November 20, 2009. Accepted November 25, 2009.
*Corresponding author.

than the cartesian forms. So, we transform the cartesian coordinates into the polar coordinates.

Let $f(x,y)$ be an input field such that it can be separated as $f(x,y) = f_1(x)f_2(y)$, where f_1 and f_2 are independent functions. Then its two-dimensional Fourier transform $\widehat{f}$ is also separable as the same symmetry property is transposed through a linear FT. Hence, $\widehat{f}(u,v) = \widehat{f_1}(u)\widehat{f_2}(v)$.

Changing to the polar coordinates and if $f(r,\theta) = f(r)$ is axially symmetrical, then in [8], it was shown that

$$\widehat{f}(k,\varphi) = 1/2 \int_0^\infty d(r^2) f(r) J_0(kr) \equiv F_0(k), \tag{1}$$

which is also axially symmetrical in the Fourier frequency domain, where F_0 is the Hankel transform of order zero. The general Hankel transform pair with the kernel being J_υ is defined as

$$F_\upsilon(p) = \int_0^\infty r f(r) J_\upsilon(pr)\, dr, \tag{2}$$

and HT being self reciprocal, its inverse is given by

$$f(r) = \int_0^\infty p F_\upsilon(p) J_\upsilon(pr)\, dp, \tag{3}$$

where $J_\upsilon(p)$ is the υ th-order Bessel function of first kind [35].

The Hankel transform arises naturally in the discussion of problems posed in cylindrical coordinates and hence, as a result of separation of variables, involving Bessel functions. The Hankel transform is frequently used as a tool for solving numerous scientific problems. It is widely used in several fields like, elasticity [19], optics [3,20,28], electromagnetics, seismology [26], astronomy and image processing [5,6,14,15,17,18,22,36]. The Hankel transform becomes very useful in analysis of wave fields where it is used in mathematical handling of radiation, diffraction, and field projection. Recently, it has been utilized to study pseudo-differential operators. Singh and Pandey [32] used HT of order υ, $\upsilon \in \mathbf{R}$ to study a special class of pseudo-differential operator (PDO) $(-x^{-1}D)^\upsilon, D = d/dx$ and proved that the (PDO) is almost an inverse of HT operator h_υ in the sense that $h_\upsilon o(-x^{-1}D)^\upsilon(\varphi) = h_0(\varphi)$ over certain Freshet space, thus representing the PDO as a Fourier-Bessel series. Further, in 1995, Singh[31], using the HT representation of the PDO, proved that $\exp^{-\alpha x^2}$, Re $\alpha > 0$ are the eigenfunctions and $\exp^{-x^2/2}$ is a fixed point of $(-x^{-1}D)^\upsilon$,$\upsilon \in \mathbf{C}$.

Several papers have been written to the evaluation of the Hankel transform in general and the zeroth order in particular. Analytical evaluations of (2) and (3) are rare and their numerical computations are difficult because of the oscillatory behavior of the Bessel function and the infinite length of the interval. Since seminal work by Siegman [30] in 1977, a number of algorithms for the numerical evaluation of the Hankel transform have been published for both zero-order [2-4,6,9,14,15,20-22,38] and high-order [1,10,16,23-25,27,37] Hankel transform. Unfortunately, the efficiency of a method for computing Hankel transform is

highly dependent on the function to be transformed, and thus it is difficult to choose the optimal algorithm for given function. In [4], the authors used Filon quadrature Philosophy to evaluate zero-order Hankel transform. They separated the integrand into the product of (assumed) slowly varying component and a rapidly oscillating one (in this case, former is $rf(r)$ and the later is $J_\upsilon(pr)$. This method works quite well for computing $F_0(p)$, for $p \geq 1$, but the calculation of inverse Hankel transform is more difficult, as $F_0(p)$ is no longer a smooth function but a rapidly oscillating one. In 1998, Yu et al. [38] gave another method to compute zero-order quasi discrete HT by approximating the input function by a Fourier-Bessel series over a finite integration interval. It lead to a symmetric transformation matrix for the HT and the IHT that satisfies the discrete form of the Parseval theorem.
Later in 2004, Guizar-Sicairos et al. [13] obtained a powerful scheme to calculate the HT of order υ by extending the zero-order HT algorithm of Yu [38] to higher orders. Their algorithm is based on the orthogonality properties of Bessel functions. Postnikov [27] proposed, for the first time, a novel and powerful method for computing zero and first order HT by using Haar wavelets.
Refining the idea of Postnikov [27], we [33-34] obtained three efficient algorithms for numerical evaluation of HT of order $\upsilon > -1$ using linear Legendre multiwavelets, Legendre wavelets and rationalized Haar wavelets which are superior to the other mentioned algorithms.
All these algorithms depend on separating the integrand $rf(r)J_\upsilon(pr)$ into two components; the slowly varying components $rf(r)$ and the rapidly oscillating component $J_\upsilon(pr)$. Then either $rf(r)$ is expanded into various wavelet series using different orthonormal bases like Haar wavelets, linear Legendre multiwavelets, Fourier Bessel series and truncating the series at an optimal level or approximating $rf(r)$ by a quadratic over the subinterval using the Filon quadrature philosophy.
But none of these algorithms were tested for the stability with respect to the noise in the input field (signal) $f(r)$ when measured experimentally. Thus it is desirable to have algorithms stable under random noise in the input field. This is the motivation behind the present work.

In this paper, we take an entirely different approach. Instead of manipulating the simpler component $rf(r)$, we manipulate the rapidly oscillating part $J_\upsilon(pr)$, thus avoiding the complexity of evaluating integrals involving Bessel functions. We use Bernstein polynomials to approximate $J_\upsilon(pr)$ and replace it by its approximation in (2), thereby getting an efficient and stable algorithm for the numerical evaluation of the HT of order $\upsilon > -1$. Test functions with known analytic HT are used with random noise term $\epsilon\theta_i$ added to the input field $f(r)$, where θ_i is a uniform random variable with values in [-1, 1], to illustrate the stability and efficiency of the proposed algorithm.

2. The Bernstein polynomials

A Bernstein polynomial, named after Sergei Natanovich Bernstein, is a polynomial in the Bernstein form that is a linear combination of Bernstein basis polynomials.
The Bernstein basis polynomials of degree n are defined by

$$B_{i,n}(t) = \binom{n}{i} t^i (1-t)^{n-i}, \quad for\ i = 0, 1, 2, ..., n. \tag{4}$$

There are $(n+1)n^{th}$ degree Bernstein basis polynomials forming a basis for the linear space v_n - consisting of all polynomials of degree less than or equal to n in $\mathbf{R[x]}$-the ring of polynomials over the field $\mathbf{R}$. For mathematical convenience, we usually set $B_{i.n} = 0$ if $i < 0$ or $i > n$.
Any polynomial $B(x)$ in $\mathbf{R[x]}$ may be written as

$$B(x) = \sum_{i=0}^{n} \beta_i B_{i,n}(x), \quad for\ some\ n. \tag{5}$$

Then $B(x)$ is called a polynomial in Bernstein form or Bernstein polynomial of degree n. The coefficients β_i are called Bernstein or Bezier coefficients. But several mathematicians call Bernstein basis polynomials $B_{i,n}(x)$ as the Bernstein polynomials. We will follow this convention as well. These polynomials have the following properties:

$(i)B_{i,n}(0) = \delta_{i,0}$ and $B_{i,n}(1) = \delta_{i,n}$, where δ is the Kronecker delta function.

$(ii)B_{i,n}(t)$ has one root, each of multiplicity i and $n-i$, at $t = 0$ and $t = 1$, respectively.

$(iii)B_{i,n}(t) \geq 0$ for $t \in [0, 1]$ and $B_{i,n}(1-t) = B_{n-i,n}(t)$.

(iv)For $i \neq 0, B_{i,n}$ has a unique local maximum in $[0, 1]$ at $t = i/n$ and the maximum value $i^i n^{-n}(n-i)^{n-i}\binom{n}{i}$.

(v)The Bernstein polynomials form a partition of unity i.e.$\sum_{i=0}^{n} B_{i,n}(t) = 1$.

(vi)It has a degree raising property in the sense that any of the lower-degree polynomials (degree $< n$) can be expressed as a linear combinations of polynomials of degree n. We have,

$$B_{i,n-1}(t) = ((n-i)/n)B_{i,n}(t) + ((i+1)/n)B_{i+1,n}(t).$$

(vii) Let $f(x) \in C[0, 1]$- the class of continuous functions on [0,1], then

$$B_n(f)(x) = \sum_{i=0}^{n} f(i/n)B_{i,n}(x) \tag{6}$$

converges to$f(x)$ uniformly on [0,1] as $n \to \infty$.

(*viii*) Let $f(x) \in C^{(k)}[0,1]$-the class of k-times differentiable functions with $f^{(k)}$ continuous, then

$$\left\|B_n(f)^{(k)}\right\|_\infty \leq \frac{(\mathbf{n})_k}{\mathbf{n}^k} \left\|f^{(k)}\right\|_\infty \text{ and } \left\|(f)^{(k)} - B_n(f)^{(k)}\right\|_\infty \to 0 \text{ as } n \to \infty,$$

where $\|.\|_\infty$ is the sup.norm and $\frac{(\mathbf{n})_k}{\mathbf{n}^k} = (1-\frac{0}{n})(1-\frac{1}{n})...(1-\frac{k-1}{n})$ is an eigen value of B_n; the corresponding eigen function is a polynomial of degree k.

3. Outline of the algorithm

The input signal $f(r)$ representing physical fields are either zero or have an infinitely long decaying tail outside a disk of finite radius R. Hence, in many practical applications either the signal $f(r)$ has a compact support or for a given $\epsilon > 0$ there exists a $R > 0$ such that $\left|\int_R^\infty rf(r)J_v(pr)\,dr\right| < \epsilon$, which is the case if $f(r) = o(r^\eta)$, where $\eta < -\frac{3}{2}$ as $r \to \infty$. Therefore, in either case,

$$\hat{F}_v(p) = \int_0^R rf(r)J_v(pr)\,dr = \int_0^1 rf(r)J_v(pr)\,dr, (byscaling) \tag{7}$$

known as the finite Hankel transform (FHT) is a good approximation of the HT given by (2). The algorithm is efficient if f decays faster that $r^{-3/2}$ near infinity which includes the majority of input signals of physical interest. Writing $rf(r) = g(r)$ in equation (7),we get

$$\hat{F}_v(p) = \int_0^1 g(r)J_v(pr)\,dr. \tag{8}$$

As $J_v(r) \in C[0,1]$, using (6), we get

$$B_n(J_v)(r) = \sum_{i=0}^n J_v(\frac{i}{n})B_{i,n}(r) \to J_v(r)\ uniformly\ as\ n \to \infty. \tag{9}$$

Replacing $J_v(pr)$ in (8) by $B_n(J_v)(pr)$, we get a sequence of iterates

$$\hat{F}_{v,n}(p) = \int_0^1 g(r)\sum_{i=0}^n J_v(\frac{pi}{n})B_{i,n}(r)\,dr = \sum_{i=0}^n J_v(\frac{pi}{n})\int_0^1 g(r)B_{i,n}(r)\,dr. \tag{10}$$

Note that the integral $\int_0^1 g(r)B_{i,n}(r)\,dr$ appearing in (10) is easy to evaluate, as $g(r)$ is the known function $rf(r)$ and $B_{i,n}(r)$ is a polynomial of degree n. We have used Mathcad 13 to evaluate (10) and plot the various graphs in Section 4. These iterates $\hat{F}_{v,n}(p) \to \hat{F}_v(p)$ uniformly as $n \to \infty$.

Let $\epsilon_n(p)$ be the associated error when we approximate $\hat{F}_v$ by its n^{th} iterate $\hat{F}_{v,n}$. Thus

$$\epsilon_n(p) = \hat{F}_{v,n}(p) - \hat{F}_v(p).$$

Let

$$\epsilon_{n,m}(p) = \epsilon_n(p) - \epsilon_m(p) = \hat{F}_{v,n}(p) - \hat{F}_{v,m}(p). \tag{11}$$

Therefore, from equations (10) and (11), we obtain

$$\epsilon_{n,n-1}(p) = \int_0^1 g(r)[\sum_{i=0}^{n} J_v(\frac{pi}{n})B_{i,n}(r) - \sum_{i=0}^{n-1} J_v(\frac{pi}{n-1})B_{i,n-1}(r)]\,dr. \tag{12}$$

For convenience of calculations, we denote the bracketed expression in (12) by $T_n(r)$. Now, we use the degree raising property of the Bernstein polynomials to express any lower degree Bernstein polynomials (degree$<n$) as a linear combination of Bernstein polynomials of degre n. In particular, any Bernstein polynomial of degree $n-1$ can be written as a linear combination of Bernstein polynomials of degree n. Using the definition of the Bernstein polynomials and simple algebraic manipulations, we obtain

$$B_{i,n-1}(r) = (\frac{n-i}{n})B_{i,n}(r) + (\frac{i+1}{n})B_{i+1,n}(r). \tag{13}$$

Substituting (13) in $T_n(r)$ and simplifying, we get

$$T_n(r) = \sum_{i=1}^{n-1}[(J_v(\frac{pi}{n}) - J_v(\frac{pi}{n-1})) - \frac{i}{n}((J_v(\frac{pi}{n-1}) - J_v(\frac{p(i-1)}{n-1}))]B_{i,n}(r) \tag{14}$$

For any $\epsilon > 0$, from the continuity of J_v there exist a $\delta > 0$ such that

$$\left|J_v(\tfrac{pi}{n}) - J_v(\tfrac{pi}{n-1})\right| < \tfrac{\epsilon}{\|g\|_\infty}$$

and

$$\left|J_v(\frac{pi}{n-1}) - J_v(p\frac{i-1}{n-1})\right| < \frac{\epsilon}{\|g\|_\infty},\ for\ n > \frac{P}{\delta} \tag{15}$$

where p is restricted to the range [0,P] and $\|g\|_\infty$ is the sup. norm of g defined as

$$\|g\|_\infty = \sup_{0\le r\le 1} |g(r)|\,. \tag{16}$$

Hence,

$$|T_n(r)| \le \frac{\epsilon}{\|g\|_\infty}[\sum_{i=1}^{n-1}(1-\frac{i}{n})B_{i,n}(r)]. \tag{17}$$

Substituting (17) in (12), we get

$$|\epsilon_{n,n-1}(p)| \le \frac{\epsilon}{\|g\|_\infty}\int_0^1 \left|g(r)\sum_{i=1}^{n-1}(1-\frac{i}{n})B_{i,n}(r)\,dr\right| \le \frac{n-1}{2(n+1)}\epsilon, \tag{18}$$

since, $\int_0^1 B_{i,n}(r)\,dr = \frac{1}{n+1}$.
As the right side of the inequality in (18) is independent of p, we have

$$\|\epsilon_{n,n-1}\|_\infty \leq \frac{n-1}{2(n+1)}\epsilon < \epsilon,\ for\ n > \frac{P}{\delta}. \tag{19}$$

Thus, we see that the iterates $\hat{F}_{v,n}(p)$ form a Cauchy sequence and hence (19) establishes the uniform convergence of $\hat{F}_{v,n}(p)$ to $\hat{F}_v(p)$. Equation (19) gives an estimate for the correction term at each step of the iterates.

4. Numerical results

In this section we discuss, the implementation of our numerical method and investigate its accuracy and stability by applying it on numerical examples with known analytical HT.
In all the examples, the exact data function is denoted by $g(r)$ and the noisy data function $g^\alpha(r)$ is obtained by adding an α random error to $g(r)$ such that $g^\alpha(r_i) = g(r_i) + \alpha\theta_i$, where $r_i = ih,\ i = 1, 2, ...N,\ Nh = 20$ and θ_i is a uniform random variable with values in [-1,1] such that $\max_{0\leq i\leq N} |g^\alpha(r_i) - g(r_i)| \leq \alpha$.
The following examples are solved with and without random perturbations to illustrate the efficiency and stability of our method by choosing three different values of the random error α as $\alpha_0 = 0.000, \alpha_1 = 0.004$ and $\alpha_2 = 0.0099$ and computing the error $E_j(p)$= Approximate HT obtained from (10) with random error α_j - the exact HT, $j = 0, 1, 2$. The various $E_j(p)'s$ are shown in Figs. 2-3,5-6,8-9,11-12 and 14-15. Note that the various graphs in the following examples are plotted by choosing the sample points as $p = 0.01(0.01)P$, where $P = 20$ in Figs. 1-15. We take $n = 80$ in (10) to get approximate solutions of the numerical examples given in this section.
We also use the continuous L^2 norm in $I = [0, P]$ to measure errors as well. It is defined as:

$$\|f\|_2 = (\int_0^P |f(r)|^2\ dr)^{1/2}. \tag{20}$$

Example 1: Sombrero function

A very important, and often used function, is the Circ function that can be defined as

$$Circ(r/a) = \begin{cases} 1 & \text{if } r \leq a, \\ 0 & \text{if } r > a \end{cases}. \tag{21}$$

The zeroth-order HT of $Circ(r/a)$ is the Sombrero function [29], given by
$S_0(p) = a^2 \frac{J_1(ap)}{ap}$.

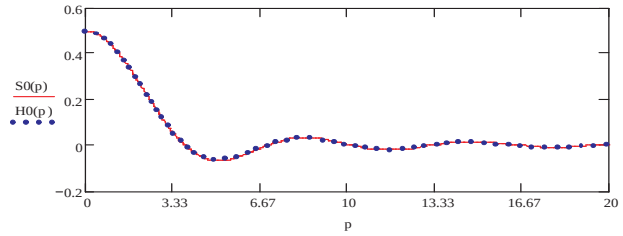

Fig.1. The exact transform, $S0(p)$ ((solid line) and the approximate transform, $H0(p)$ (dotted-line).

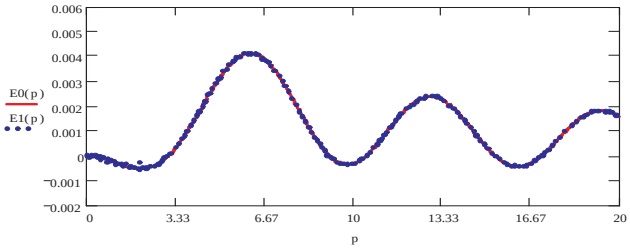

Fig.2. Errors $E0(p)$ (with $\alpha_0 = 0$, solid line) and $E1(p)$ (with $\alpha_1 = 0.004$, dotted line).

We use (10) to obtain the approximation for the FHT $\hat{F_0}(p)$ of the $Circ(r/a)$ and compare it with the exact HT $S0(p)$ in Fig 1. Note that $S0(p)$ and $\hat{F_0}(p)$ are indicated by $S0(p)$ (solid line) and $H0(p)$ (dotted line) in the Fig.1.The effect of random noises are shown through Figs.2 and 3 where the error $E0(p)$ (without noise) is compared with the errors $E1(p)$ and $E2(p)$, with different levels of random noises, respectively.

Example 2:

Let $f(r) = (1 - r^2)^{1/2},\ 0 \leq r \leq 1,$
then,

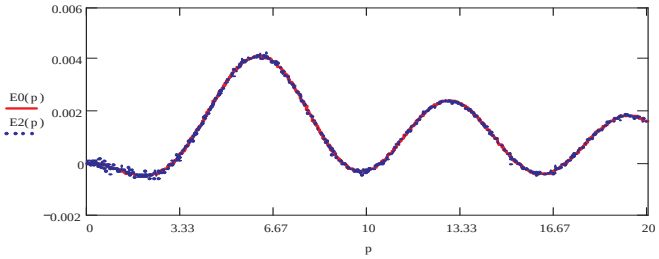

Fig.3. Errors $E0(p)$ (with $\alpha_0 = 0$, solid line) and $E2(p)$ (with $\alpha_2 = 0.0099$, dotted line).

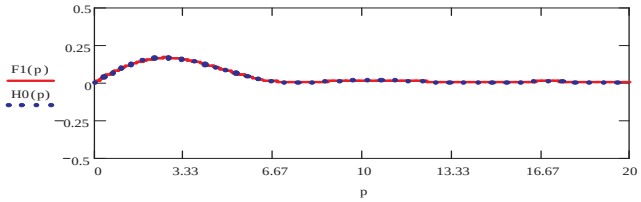

Fig.4.The exact transform, $F1(p)$ ((solid line) and the approximate transform, $H0(p)$ (dotted-line).

$$F_1(p) = \begin{cases} \pi \frac{J_1^2(p/2)}{2p} & \text{if } 0 < p < \infty, \\ 0 & \text{if } p = 0 \end{cases} . \tag{22}$$

Barakat et al. [4], evaluated $F_1(p)$ numerically using Filon quadrature philosophy but the associated error is appreciable for $p < 1$; whereas our method gives almost zero error in that range. Equation (10) is used to find the approximate FHT for the problem. The comparison of the approximation $H0(p)$ (dotted line) with the exact HT $F1(p)$ (solid line) is shown in Fig.4 and the corresponding error graphs,$(E0(p), E1(p))$ and $(E0(p), E2(p))$ in Figs 5 and 6 respectively.

Example 3:

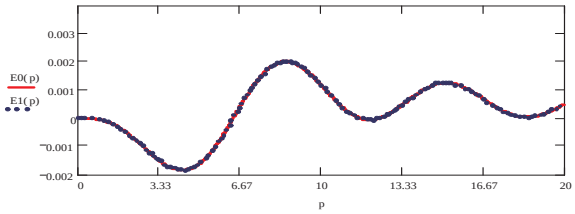

Fig.5. Errors $E0(p)$ (with $\alpha_0 = 0$, solid line) and $E1(p)$ (with $\alpha_1 = 0.004$, dotted line).

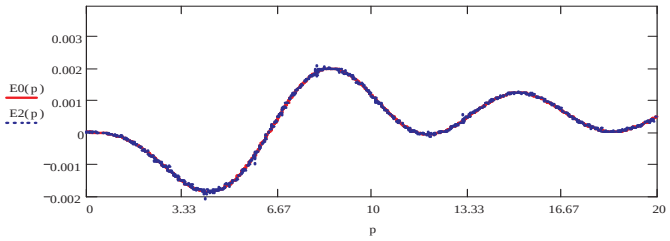

Fig.6. Errors $E0(p)$ (with $\alpha_0 = 0$, solid line) and $E2(p)$ (with $\alpha_2 = 0.0099$, dotted line).

Let $f(r) = \frac{2}{\pi}[\arccos(r) - r(1-r^2)^{1/2}]$, $0 \le r \le 1$,
then

$$F_0(p) = 2\frac{J_1^2(p/2)}{p^2},\ 0 \le p \le \infty.\ [2] \tag{23}$$

A well known result. The pair $(f(r), F_0(p))$ arises in optical diffraction theory [11]. The function $f(r)$ is the optical transfer function of an aberration-free optical system with a circular aperture, and $F_0(p)$ is the corresponding spread function.

Barakat et al. [2], evaluated $F_0(p)$ numerically using Filon quadrature philosophy but the associated error is again appreciable for $p < 1$; whereas our method gives almost zero error in that range. Note that $F_0(p)$ and $\hat{F_0}(p)$ are indicated by $F0(p)$ (solid line) and $H0(p)$ (dotted line) in the Fig.7 and the corresponding errors $(E0(p), E1(p))$ and $(E0(p), E2(p))$ are shown in Figs. 8 and 9 respectively.

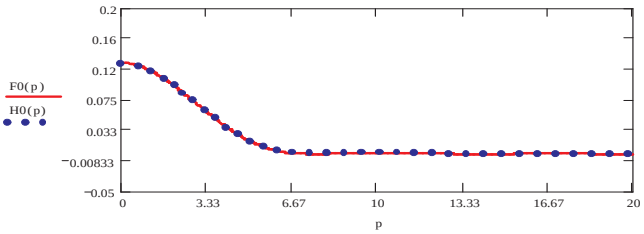

Fig.7.The exact transform,$F0(p)$((solid line) and the approximate transform,$H0(p)$ (dotted-line)

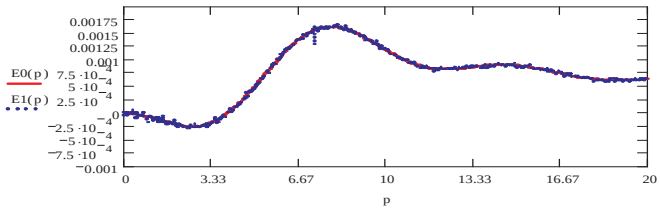

Fig.8. Errors $E0(p)$ (with $\alpha_0 = 0$, solid line) and $E1(p)$ (with $\alpha_1 = 0.004$, dotted line).

Example 4.

In this example, we choose as test function the generalized version of the top-hat function, $f(r) = r^{\upsilon}[H(r) - H(r-a)],\ a > 0$ where $H(r)$ is the step function given by

$$H(r) = \begin{cases} 1 & \text{if } r \geq 0, \\ 0 & \text{if } r < 0 \end{cases}.$$

Then

$$F_{\upsilon}(p) = \frac{J_{\upsilon+1}(p)}{p}. \tag{24}$$

In [13], authors took $a = 1$ and $\upsilon = 4$ for numerical calculations. We take $a = 1$, $\upsilon = 1/2$ and observe that the associated errors with and without random noises are quite small as shown in Figs. 11 and 12. The comparison of the

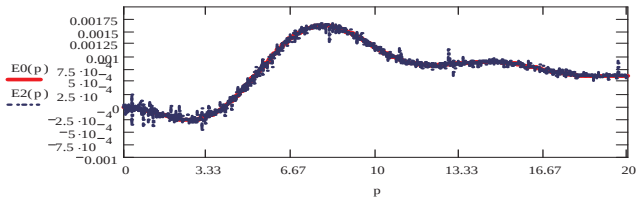

Fig.9. Errors $E0(p)$ (with $\alpha_0 = 0$, solid line) and $E2(p)$ (with $\alpha_2 = 0.0099$, dotted line).

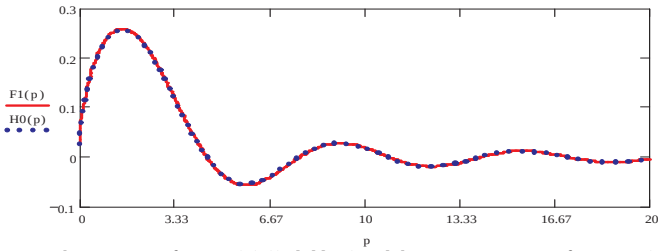

Fig.10.The exact transform, $F1(p)$ ((solid line) and the approximate transform, $H0(p)$ (dotted-line).

approximation with exact transform is shown in Fig.10 where the exact and approximate transforms are denoted as $S1(p)$ (solid line) and $H0(p)$ (dotted line) respectively.

Example 5:

Let $f(r) = r^{\upsilon} \sin(\frac{\pi r^2}{4})$, $0 \leq r \leq 1$, then

$F_{\upsilon}(p) = \frac{1}{\sqrt{2}}(\frac{\pi}{2})^{-\upsilon-1} p^{\upsilon}[U_{\upsilon+1}(\frac{\pi}{2}, p) - U_{\upsilon+2}(\frac{\pi}{2}, p)]$ (obtained from [7, p.34 Eq(16)] by putting $a = \frac{\pi}{4}$, $b = 1$), where $U_{\upsilon}(w, p)$ is a Lommel's function of two variables,

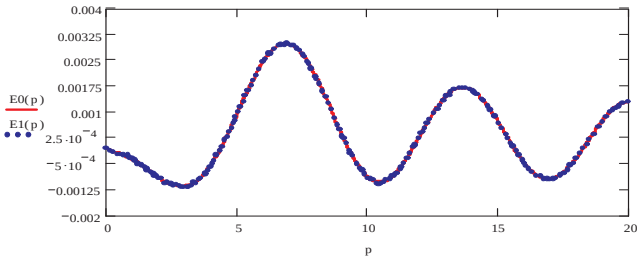

Fig.11. Errors $E0(p)$ (with $\alpha_0 = 0$, solid line) and $E1(p)$ (with $\alpha_1 = 0.004$, dotted line).

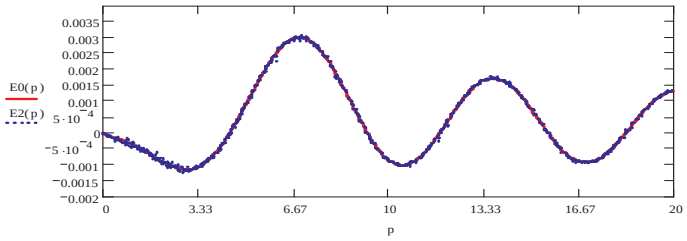

Fig.12. Errors $E0(p)$ (with $\alpha_0 = 0$, solid line) and $E2(p)$ (with $\alpha_2 = 0.0099$, dotted line).

$$= \frac{1}{\sqrt{2}p}[\sum_{\eta=0}^{L}[(-1)^{\eta}(\frac{\pi}{2p})^{2\eta}(J_{\upsilon+2\eta+1}(p) - \frac{\pi}{2p}J_{\upsilon+2\eta+2}(p))]] \; as \; L \to \infty. \; [7, p.428] \tag{25}$$

We take $\upsilon = 1.5$ and show the comparison of the approximation $H0(p)$ (dotted line) with the exact HT $F_{1.5}(p)$ (solid line) in Fig.13.The corresponding errors $(E0(p), E1(p))$ and $(E0(p), E2(p))$ are shown in Figs 14 and 15 respectively.

5. Error Analysis

The numerical stability property of the algorithm is illustrated in table 1 where the L^2 norm of the error is shown as a function of the amount of noise ϵ in the data function, for Examples 1- 5. We notice that in all the cases, the numerical stability of the proposed algorithm is confirmed. Moreover, in the α

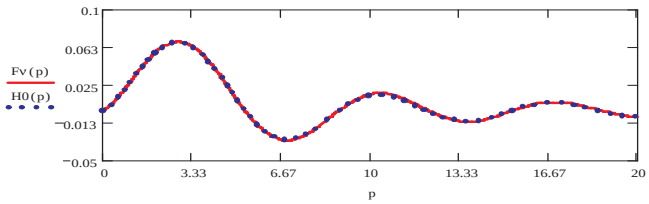

Fig.13.The exact transform, $Fv(p)$ ($v = 1.5$, solid line) and the approximate transform, $H0(p)$ (dotted-line).

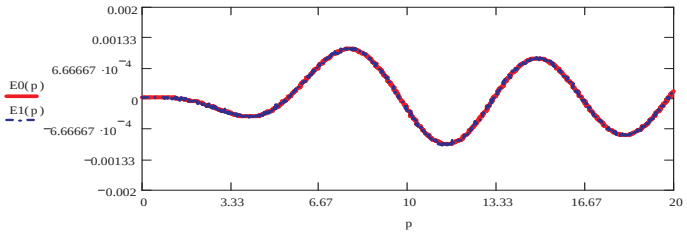

Fig.14. Errors $E0(p)$ (with $\alpha_0 = 0$, solid line) and $E1(p)$ (with $\alpha_1 = 0.004$, dotted line).

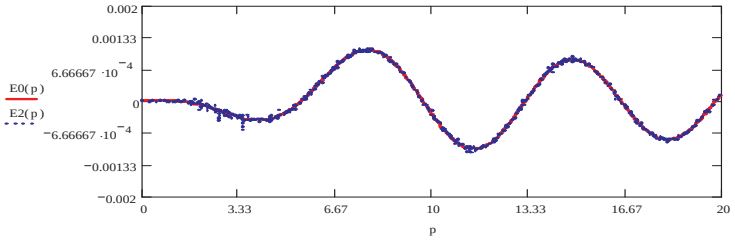

Fig.15. Errors $E0(p)$ (with $\alpha_0 = 0$, solid line) and $E2(p)$ (with $\alpha_2 = 0.0099$, dotted line).

range 0.000 to 0.0099, the continuous error norms are barely sensitive to the variation in α.

$\|E_j\|_2$	$Ex.1.$	$Ex.2.$	$Ex.3.$	$Ex.4.$	$Ex.5.$
$\|E_0\|_2$	7.924×10^{-3}	4.62×10^{-3}	3.999×10^{-3}	5.675×10^{-3}	2.585×10^{-3}
$\|E_1\|_2$	7.937×10^{-3}	4.627×10^{-3}	4.004×10^{-3}	5.659×10^{-3}	2.595×10^{-3}
$\|E_2\|_2$	7.916×10^{-3}	4.671×10^{-3}	4.001×10^{-3}	5.673×10^{-3}	2.64×10^{-3}

Table 1: Least squares errors $\|E_j\|_2$, for $j = 0, 1, 2$ $Exs.1 - 5$.

6. Conclusions

Replacing the rapidly oscillating part $J_\upsilon(pr)$ with its approximation by Bernstein polynomials avoids the complexity of evaluating integrals involving Bessel functions. This makes the evaluation of HT integral very simple. From Figs.1-15, it is obvious that the method is consistent and does not depend on the particular choice of the input signals. The stability of the proposed algorithm is established through Figs 2-3, 5-6, 8-9, 11-12, 14-15 and table 1.The accuracy and simplicity of the algorithm provides it an edge over the others.

References

1. A. Agnesi, G.C. Reali, G. Patrini and A. Tomaselli, *Numerical evaluation of the Hankel transform: remarks*,J. Opt. Soc. Am. A **10** (1993),1872-1874.
2. R. Barakat and E. Parshall, *Numerical evaluation of the zero-order Hankel transform using Filon quadrature philosophy*, Appl. Math. Lett. **9** (1996), 21-26.
3. R. Barakat, E. Parshall and B.H. Sandler, *Zero-order Hankel transform algorithms based on Filon quadrature philosophy for diffraction optics and beam propogation*,J. Opt. Soc. Am. A **15** (1998), 652-659.
4. R. Barakat and B.H. Sandler, *Evaluation of first-order Hankel transforms using Filon quadrature Philosophy*, Appl. Math. Lett. **11** (1998), 127-131.
5. S.M. Candel, *Dual algorithms for fast calculation of the Fourier Bessel transform*,IEEE Trans. Acoust. Speech Signal Process ASSP- **29** (1981), 963-972.
6. E.C. Cavanagh and B.D.Cook , *Numerical evaluation of Hankel Transform via Gaussian-Laguerre polynomial expressions*,IEEE Trans. Acoust. Speech Signal Process ASSP- **27** (1979), 361-366.
7. A. Erdelyi(Ed.), *Tables of Integral Transforms*,McGraw-Hill, New York (1954).
8. H.Y. Fan, *Hankel transform as a transform between two entangled state representations*, Phys. Lett. A **313** (2003), 343-350.
9. J.A. Ferrari, *Fast Hankel transform of order zero*, J. Opt. Soc. Am. A **12** (1995), 1812-1813.
10. J.A. Ferrari, D. Peciante and A. Durba, *Fast Hankel transform of nth order*,J. Opt. Soc. Am. A **16** (1999),2581-2582.
11. J. Gaskell, *Linear systems, Fourier transforms, and Optics, chapter 11*,Wiely, New York (1978).
12. J.W. Goodman, *Introduction to Fourier Optics*, McGraw-Hill, New York , 1968.
13. M. Guizar-Sicairos and J.C. Gutierrez-Vega, *Computation of quasi-discrete Hankel transforms of integer order for propagating optical wave fields* ,J. Opt. Soc. Am. A **21** (2004),53.
14. E.V. Hansen, *Fast Hankel transform algorithms*,IEEE Trans. Acoust. Speech Signal Process ASSP- **33** (1985), 666-671.

15. E.V. Hansen, *Correction to Fast Hankel transform algorithms*,IEEE Trans. Acoust. Speech Signal Process ASSP- **34** (1986), 623-624.
16. W.E. Higgins and D.C. Munsons Jr., *An algorithm for computing general integer order Hankel Transforms*,IEEE Trans. Acoust. Speech Signal Process ASSP- **35** (1987), 86-97.
17. W.E. Higgins and D.C. Munsons Jr., *A Hankel transform approach to tomographic image Reconstruction*, IEEE Trans. Med. Imag. **7** (1988), 59-72.
18. L. Knockaret, *Fast Hankel transform by fast sine and cosine transform: the Mellin connection*,IEEE Trans. Signal Process **48** (2000), 1695-1701.
19. V.S. Kulkarni and K.C. Deshmukh , *An inverse quasi-static steady-state in a thick circular plate*, J. Frank. Inst **345** (2008), 29-38.
20. V. Magni, G. Cerullo and D. Silvestri, *High-accuracy fast Hankel transform for optical beam Propagation*,J. Opt. Soc. Am. A **12** (1992), 2031-2033.
21. J. Markham and J.A. Conchello, *Numerical evaluation of Hankel transform for oscillating Function*,J. Opt. Soc. Am. A **20** (2003), 621-630.
22. D.R. Mook, *An algorithm for numerical evaluation of Hankel and Abel transform*, IEEE Trans. Acoust. Speech Signal Process ASSP- **31** (1983), 979-985.
23. P.K. Murphy and N.C. Gallagher, *fast algorithm for computation of zero-order Hankel transform*,J. Opt. Soc. Am. **73** (2003), 1130-1137.
24. A.V. Oppenheim, G.V. Frish and D.R. Martinez, *An algorithm for numerical evaluation of Hankel transform*,IEEE Proc.**66** (1980), 264-265.
25. A.V. Oppenheim, G.V. Frish and D.R. Martinez, *Component of Hankel transform using projections* ,J. Acoust. Soc. Am. **68** (1980), 523-529.
26. D. Patella, *Gravity interpretation using the Hankel transform*, Geophysical Prospecting **28** (1980), 744-749.
27. E.B. Postnikov, *About calculation of the Hankel transform using preliminary wavelet transform*,J. Appl. Math. **6** (2003),319-325.
28. J.J. Reis, R.T. Lynch and J. Butman, *Adaptive Harr transform video bandwith reduction stem for RPV's, in* Proceeding of the annual meeting on society of Photo Optic Instrumentation Enginering (SPIE),San Diego, CA (1976), 24-45.
29. J.D. Secada, *Numerical evaluation of the Hankel transform*,Compu. Phys. Commun. **116** (1999),278-294.
30. A.E. Siegman, *Quasi Fast Hankel Transform*, J. Optics. Lett **1** (1977), 13-15.
31. 0.P. Singh, *On pseudo-differential operator* $(-x^{-1}D)^{\upsilon}$, J. Math. Anal. Appl. **191** (1995), 450-459.
32. 0.P. Singh and J.N. Pandey, *The Fourier-Bessel series representation of the pseudo differential operator* $(-x^{-1}D)^{\upsilon}$, Proc. Amer. Math. Soc. **115** (1992), 969-976.
33. V.K. Singh,O.P. Singh and R.K. Pandey, *Numerical evaluation of Hankel transform by using linear Legendre multi-wavelets*,Compu. Phys. Commun. **179** (2008),424-429.
34. V.K. Singh,O.P. Singh and R.K. Pandey, *Efficient algorithms to compute Hankel transforms using Wavelets*,Compu. Phys. Commun. **179** (2008),812-818.
35. I. N. Sneddon, *The use of Integral Transforms*, McGraw-Hill , 1972.
36. B.W. Suter, *Fast nth order Hankel transform algorithm*,IEEE Trans. Signal Process **39** (1991), 532-536.
37. B.W. Suter and R.A. Hedges, *Understanding fast Hankel transform*,J. Opt. Soc. Am. A **18** (2001),717-720.
38. Li. Yu, M. Huang, M. Chen, W. Huang and Z. Zhu *Quasi-discrete Hankel transform*, Opt.Lett. **23** (1998), 409-411.

Om P. Singh is a Professor at the Department of Applied Mathematics, Institute of Technology, Banaras Hindu University, Varanasi, India. His area of interest are Pseudo-Differential operators,Wavelets, Integral transforms, Differential and Integral equations.

Department of Applied Mathematics, Institute of Technology, Banaras Hindu University, Varanasi, India.
e-mail:opsingh.apm@itbhu.ac.in; singhom@gmail.com

V. K. Singh and **R. K. Pandey** received their Ph.D. degrees from Institute of Technology, Banaras Hindu University in 2009. Their area of intrests are Wavelets and integral equations. They are Asst. Professors at Birla Institute of Technology and Science-Pilani, Goa Campus, Goa and PDPM Indian Institute of Information Technology, Design and Manufacturing, Jabalpur, India, respectively.